Journal of Alloys and Compounds 665 (2016) 394–403

Contents lists available at ScienceDirect

Journal of Alloys and Compounds

journal homepage: http://www.elsevier.com/locate/jalcom

Annealing temperature effect on magnetic and magnetocaloric properties of manganites

Abd El-Moez A. Mohamed [a, b, *], V. Vega [b, c], M. Ipatov [d], A.M. Ahmed [a], B. Hernando [b]

[a] Physics Department, Faculty of Science, Sohag University, Sohag 82524, Egypt
[b] Physics Department, Faculty of Science, Oviedo University, Oviedo 33007, Spain
[c] Laboratory of Nanoporous Membranes, Oviedo University, Oviedo 33006, Spain
[d] Materials Physics Department, Faculty of Chemistry, Basque Country University, San Sebastian 20018, Spain

ARTICLE INFO

Article history:
Received 4 December 2015
Received in revised form
7 January 2016
Accepted 8 January 2016
Available online 11 January 2016

Keywords:
Composite materials
Rare earth alloys and compounds
Grain boundaries
Magnetization
Magnetocaloric effect

ABSTRACT

In this work, we investigate the effect of annealing process at different temperatures (600 and 800 °C) on structural, magnetic and magnetocaloric properties of $La_{0.7}Ba_{0.3}MnO_3/xTiO_2$ system with x = 0.04 and 0.06. Crystal structure analysis shows the R-3c rhombohedral symmetry for composites in both annealing temperatures indicating structure stability. Magnetization and coercive field of doped composites increase with increasing annealing temperature, while there is no effect on their Curie temperature (T_c) that remains constant at 348 K due to the TiO_2-$La_{0.7}Ba_{0.3}MnO_3$ interaction lack. Increasing annealing temperature is found to be an effective process that can positively affect the magnetocaloric properties. Where, the relative cooling power of doped composites increases from 50 to 62 J/kg for x = 0.04 composite and from 54 to 66 J/kg for x = 0.06 composite with increasing annealing temperature from 600 to 800 °C. Moreover, the experimental results of magnetic entropy change have been modulated using Landau theory and the calculations have indicated the negligible contribution of elastic, magnetoelastic and magnetoelectronic coupling in the magnetocaloric properties of $La_{0.7}Ba_{0.3}MnO_3/xTiO_2$ system in both annealing temperatures.

1. Introduction

Magnetic refrigeration technique is one of the most promising techniques in cooling technology because of the efficient and the environmental safe cooling applications, which have encouraged the experimental and the theoretical studies in this direction. Obtaining low cost and high performance magnetocaloric materials is not an easy target because of the associated demerits. For example, Gd shows a large magnetocaloric effect (MCE) in room temperature range [1], but it is an expensive element and tends to oxidation. Current researches seek to balance the needs of technical applications by obtaining high MCE performance with fewer disadvantages by investigating various kinds of magnetic materials treated in different conditions.

Recently, manganites oxides have been paid attention for MCE applications because of the outstanding physico-chemical properties that enable them to work with chemical stability and high magnetization. The *magnetoresistive/insulator* system is an inhomogeneous system consisting of non-reacted manganite and insulator materials such as $La_{0.7}Sr_{0.3}MnO_3/ZrO_2$ [2]. The main idea behind this system depends on the interaction lack between manganite and insulator materials that keeps on the intrinsic properties of the manganite material. This enables us to tune the T_c related phenomena as the MCE at the same temperature range [3]. In fact, the insulator distribution at the grain boundaries and on the surface of the manganite grains is the key role of this system properties. For instance, the insulator distribution changes the boundaries resistance that increases magnetization disconnection leading to the spin tunneling between grains and hence to the low field magnetoresistance [4]. The insulator distribution may be affected by annealing temperature modifying magnetic properties

* Corresponding author. Physics Department, Faculty of Science, Oviedo University, Oviedo 33007, Spain.
E-mail address: abdmoez_hussien@science.sohag.edu.eg (A.A. Mohamed).

http://dx.doi.org/10.1016/j.jallcom.2016.01.057
0925-8388/

and related phenomena. Accordingly, after we have studied the effect of insulator doping level in $La_{0.7}Ba_{0.3}MnO_3/xTiO_2$ system ($0 \leq x \leq 0.08$) in a previous study [3] and managed to enhance the MCE of $La_{0.7}Ba_{0.3}MnO_3$ at the same temperature range, it is a fruitful to study the influence of insulator distribution by annealing temperature and its effect on magnetic and magnetocaloric properties of $La_{0.7}Ba_{0.3}MnO_3/xTiO_2$ system that has not been knocked before in these systems.

2. Experimental method

Polycrystalline $La_{0.7}Ba_{0.3}MnO_3/xTiO_2$ ceramic samples with x = 0.04 and 0.06 composites were prepared in several steps. $La_{0.7}Ba_{0.3}MnO_3$ (LBMO) was prepared by the sol-gel method using $LaN_3O_9.6H_2O$, Ba $(OOCCH_3)_2$ and Mn $(OOCCH3)_2.4H_2O$ raw as reported in Ref. [5] and sintered at 1200 °C for 24 h. TiO_2 nanotubes (NTs) were prepared by the electrochemical anodization method of titanium foils (99.6%) as reported in Ref. [6]. Then, the resultant TiO_2 NTs were annealed for 2 h at 400 °C. Stoichiometric amounts of LBMO and TiO_2 were mixed and pressed, then annealed at different temperatures of 600 °C and 800 °C for 24 h. Crystal structure was examined by x-ray diffraction (XRD) at room temperature, and the patterns were analyzed using Rietveld refinement method with FULLPROF program. Surface morphology was carried out using scanning electron microscope (SEM), while, magnetic and magnetocaloric characterizations were performed using SQUID magnetometer.

Table 1
Symmetry, cell volume (V), SEM grain size (G) and XRD crystallite size (P) of LBMO/*x*TiO2 composites annealed at 600 and 800 °C.

Composition	Condition	Symmetry	V (Å)^3	G (μm)	P (nm)
x = 0	as-prepared	R-3c	358.86	0.74	32
x = 0.04	600 °C	R-3c	358.17	0.63	34
	800 °C	R-3c	358.25	0.65	33
x = 0.06	600 °C	R-3c	358.23	0.67	33
	800 °C	R-3c	358.20	0.68	34

3. Results and discussion

3.1. Structure

XRD patterns of LBMO/$xTiO_2$ composites annealed at 600 and 800 °C are shown in Fig. 1. The single phase of the undoped LBMO compound indicates the high homogeneity and the complete reaction between elements. The patterns of doped composites are characterized by an additional peak of TiO_2 at $2\theta = 25.32°$ revealing its coexistence with LBMO phase. This suggests TiO_2-LBMO interaction lack in doped composites that seems to be preserved with increasing annealing temperature due to the quite similar peak intensity of TiO_2 in both annealing temperatures. The interaction lack leads to several consequences as structure stability at the R-3c rhombohedral symmetry, cell volume (V) insignificant change and constant value of XRD crystallite size (P) for composites in both

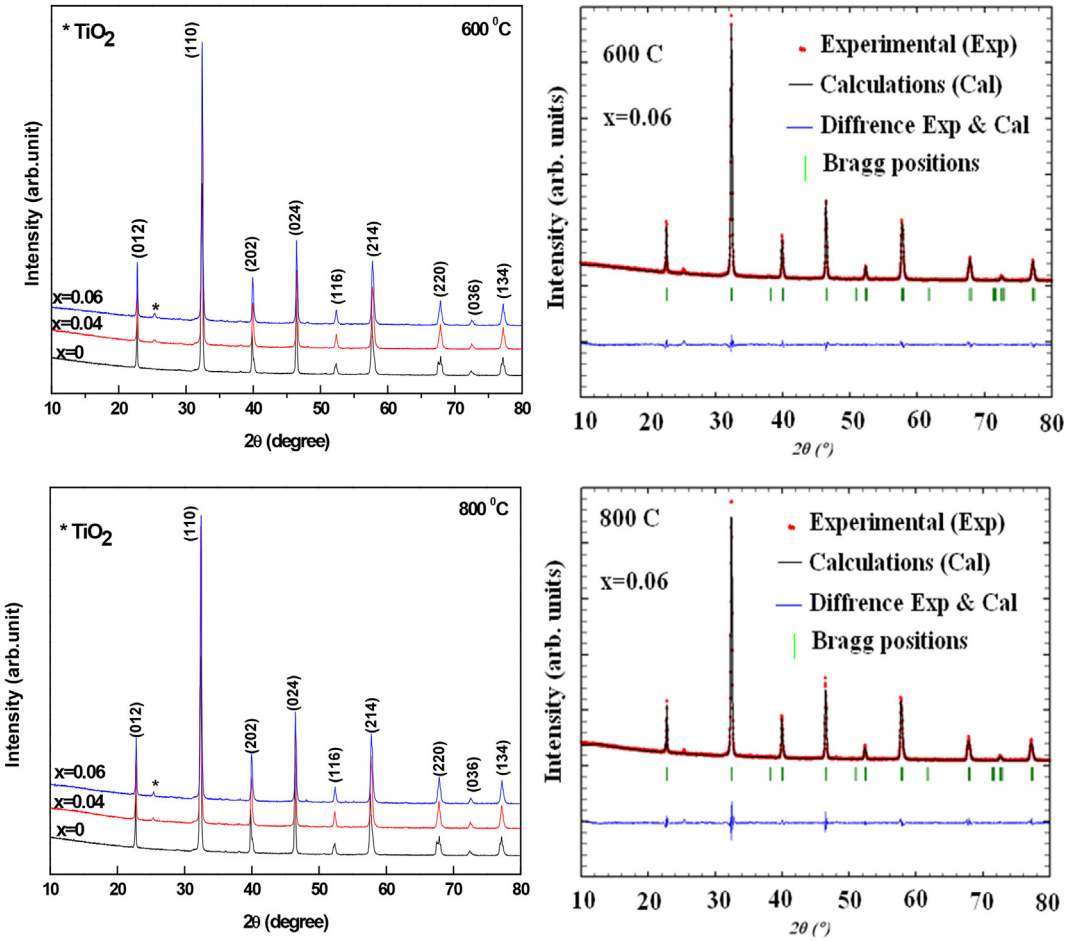

Fig. 1. XRD patterns of LBMO/$xTiO_2$ composites and Rietveld refinement profile for x = 0.06 composite annealed at 600 and 800 °C.

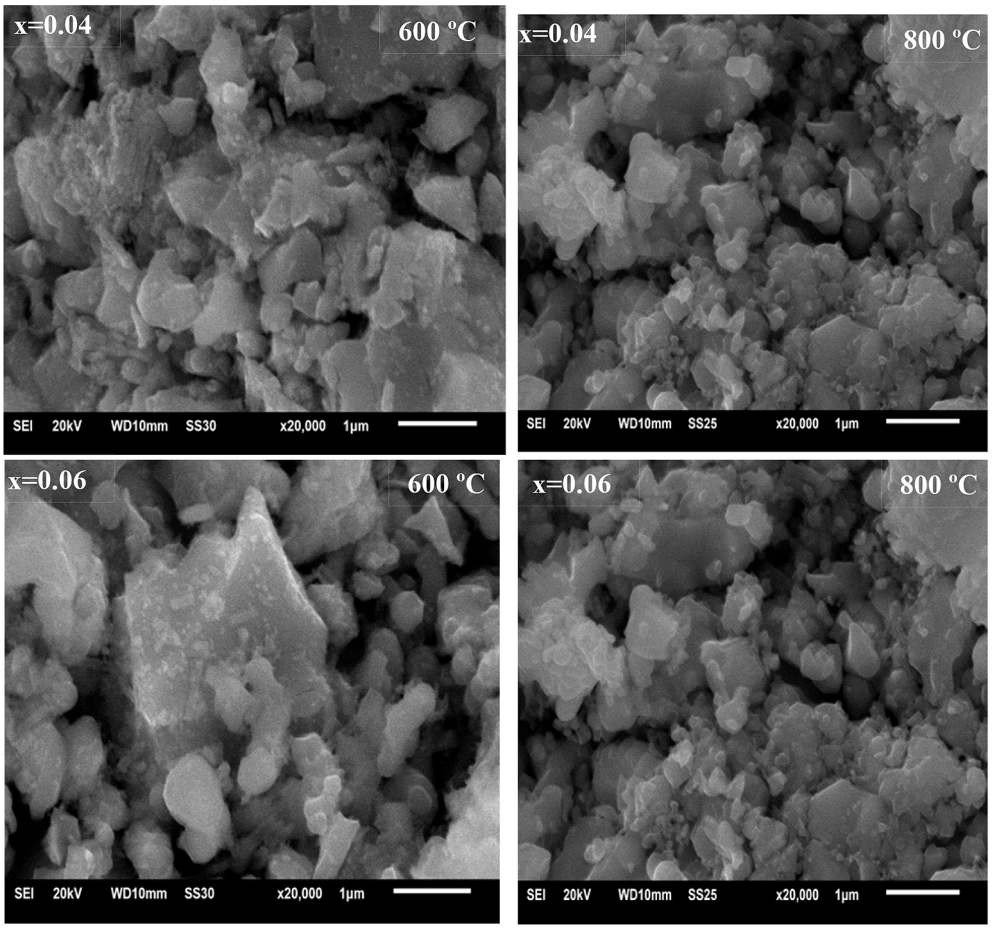

Fig. 2. SEM micrographs of LBMO/xTiO$_2$ doped composites for x = 0.04 and x = 0.06 annealed at 600 and 800 °C.

annealing temperatures as shown in Table 1. Where, P was determined by Laue-Scherrer equation and Rietveld refinement profiles of x = 0.06 composite annealed at 600 and 800 °C are displayed in Fig. 1 as a selected sample. SEM micrographs in Fig. 2 support the idea of TiO_2-LBMO interaction lack, where it show TiO_2 precipitation at the boundaries and on the surfaces of LBMO grains leading to the quite constant value of the average SEM grain size (G) in both annealing temperatures (see Table 1). In addition, this figure shows the influence of TiO_2 distribution by annealing temperature. Where, TiO_2 grains are well agglomerated and less randomized in composites annealed at the higher temperature of 800 °C in comparison with these annealed at 600 °C. Also, it is noteworthy the smaller value of XRD crystallite size compared with the SEM grain size in all annealed composites, which proposes crystallites collectivization inside the grain as a result of structural defects and/or internal stresses [7].

3.2. Magnetization

The thermal variation of magnetization at 100 Oe applied magnetic field is shown in Fig. 3a and b for composites in both annealing temperatures. The ferromagnetic-paramagnetic (FM-PM) transition is observed at the same T_c value (348 K) for all composites in both annealing temperatures, which corresponds to the T_c of the undoped LBMO reported in our work [3]. The constant behavior of T_c with doping or annealing proess is in agreement with [8,9] and refers to the TiO_2-LBMO interaction lack. This is because T_c is an intrinsic property depends only on the interior ferromagnetism of LBMO grains [10], which is kept without any change due to the interaction lack between TiO_2 and LBMO either with doping level or with increasing annealing temperature. From Fig. 3a,b we can see that the magnetization of doped composites increases with increasing annealing temperature, in agreement with [11,12]. The magnetization change with annealing temperature may be attributed to intrinsic and/or extrinsic effects. The intrinsic effect comes from a change in LBMO grain size and bandwidth [11], while, the extrinsic effect arises from grain boundaries that decrease grains connectivity, interrupt the interfacial magnetization and lead to magnetization pinning. The negligible change in grain size with annealing temperature suggests a non change in the intrinsic spin disorder [13–15] indicating the negligible role of grain size in the magnetization change. In addition, the change in LBMO bandwidth happens only in case of the partial substitution of Mn ions by Ti^{4+} ions, which is excluded in our case due to the TiO_2-LBMO interaction lack. This suggests that the magnetization change more likely arises due to the grain boundaries extrinsic effect rather than the intrinsic effects. The grain boundaries thickness and resistance increase with TiO_2 segregation [3], which in turn increase magnetization pinning. The agglomeration of TiO_2 grains seems to be enhanced with increasing annealing temperature (800 °C) as seen in Fig. 2, which decreases their random distribution at grain boundaries leading to an increase in the magnetization due to pinning decrease. Vice versa, annealing process at low temperature

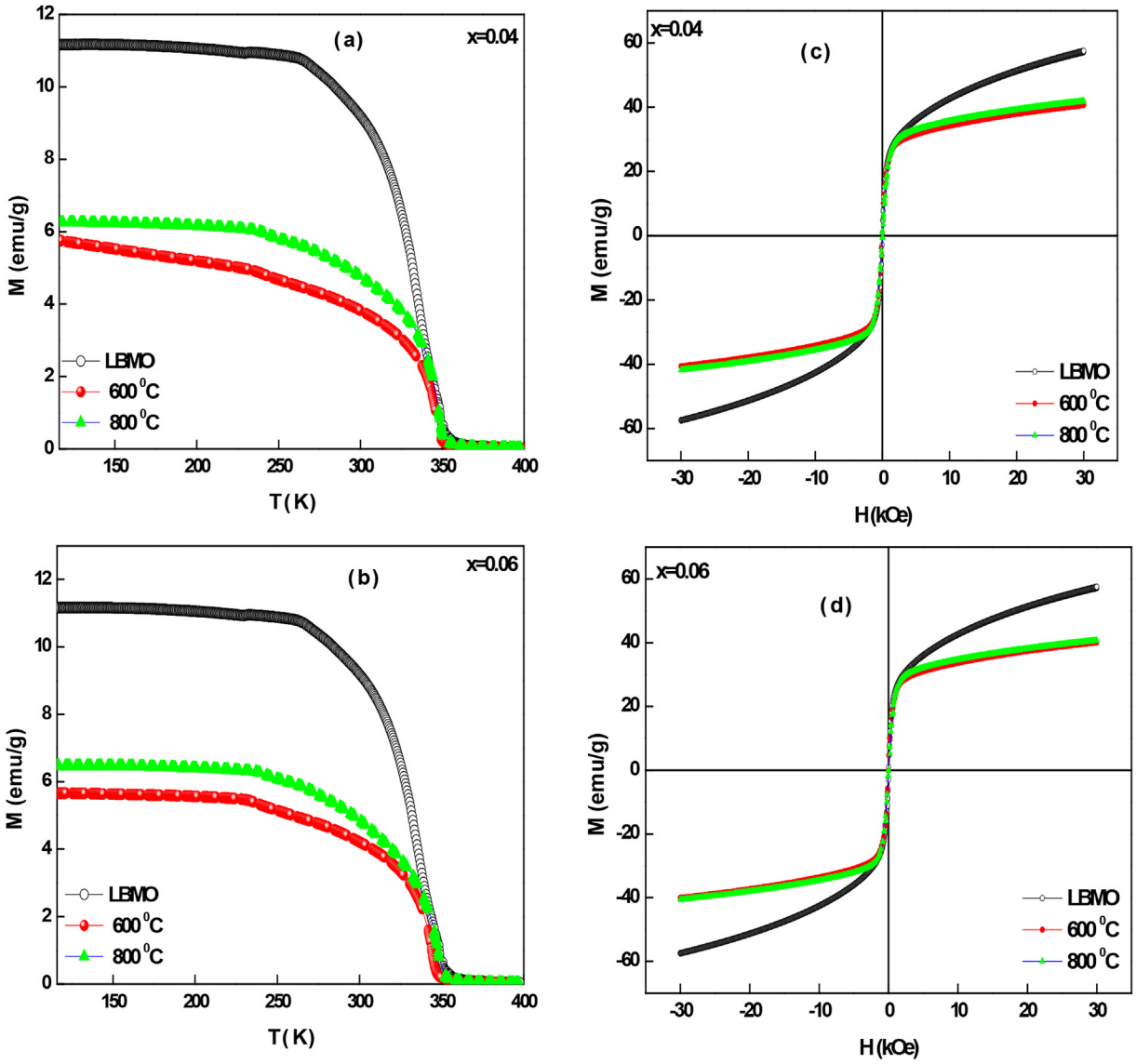

Fig. 3. (a), (b) Magnetization dependent temperature and (c), (d) hysteresis loops at 300 K for LBMO/xTiO$_2$ system doped composites annealed at 600 and 800 °C, respectively.

(600 °C) decreases TiO_2 agglomeration and increases their random distribution at grain boundaries, which decrease magnetization due to pinning increase. According to the effect of annealing temperature on TiO_2 distribution and its effect on magnetization value, results from hysteresis loops in Fig. 3c and d reveal that both composites show higher saturation magnetization (M_s) and coercive field (H_c) values at the higher annealing temperature of 800 °C, as seen Table 2, in agreement with [16]. This is as discussed before due to the better ordering and the well agglomeration of TiO_2 grains away from LBMO grain boundaries in composites annealed at 800 °C rather than these annealed at 600 °C.

Table 2
Curie temperature (T_c), saturation magnetization (M_s) and coercive field (H_c) of doped composites at 600 and 800 °C.

Composition	Condition	T_c (K)	M_s (emu/g)	H_c(Oe)
x = 0	as-prepared	348	47	50
x = 0.04	600 °C	348	33.7	40
	800 °C	348	38.4	44
x = 0.06	600 °C	348	31.3	16
	800 °C	348	35.2	31

3.3. Magnetocaloric effect (MCE)

Fig. 4 shows the isothermal magnetization curves of LBMO and doped composites annealed at 600 and 800 °C. In both annealing temperatures, the magnetization below T_c increases sharply at low magnetic fields then saturates at high magnetic fields in correspondence with the ferromagnetic behavior. While above T_c, magnetization changes linearly with the applied magnetic field as a feature of paramagnetism. The nature of FM-PM transition and its impact by annealing temperature can be identified from Arrott plots in Fig. 5. These plots indicate the second order transition for composites in both annealing temperatures because of the positive slope around T_c that characterizes the second order transition [17].

The magnetic entropy change, ΔS, was determined from the

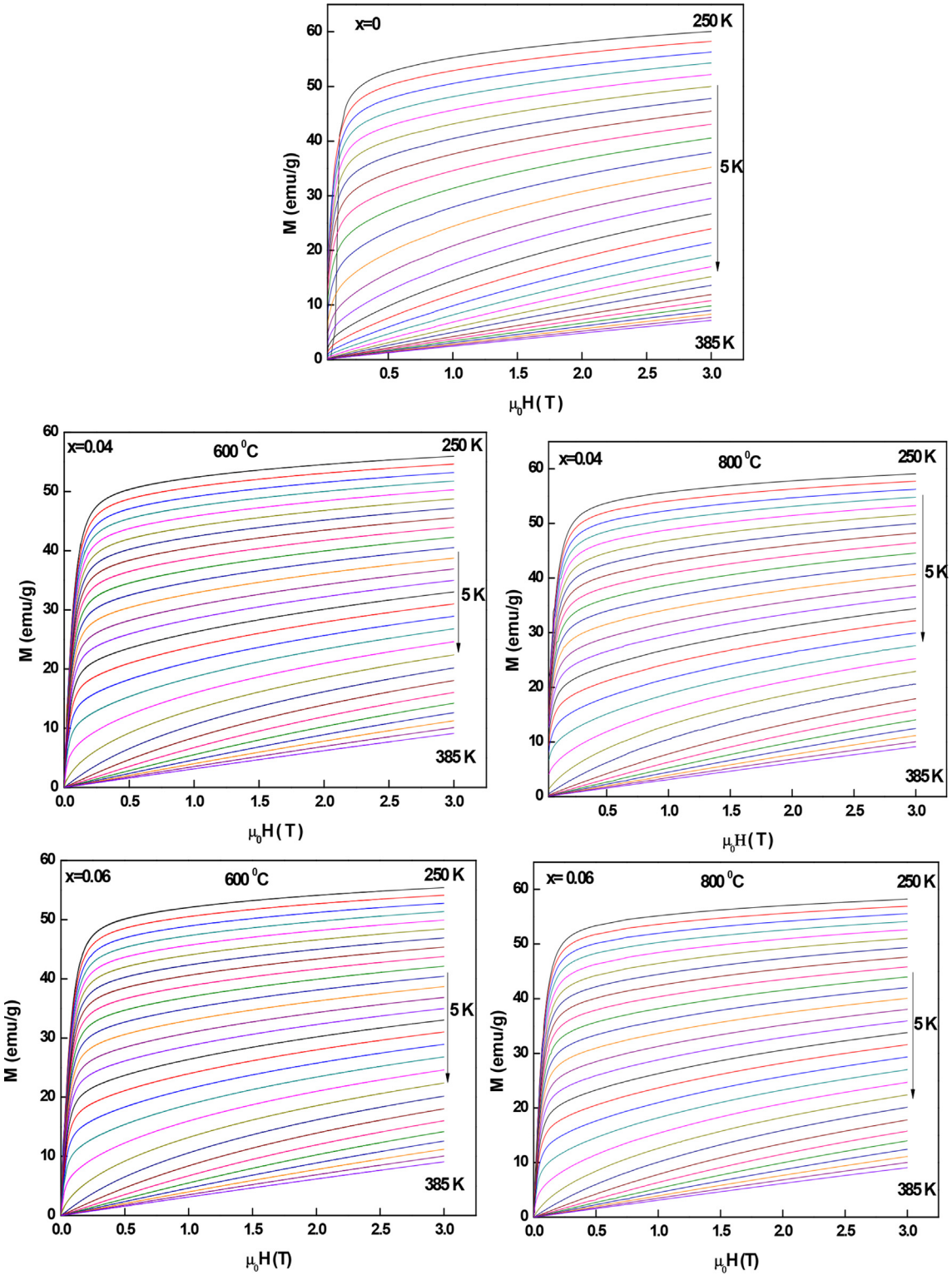

Fig. 4. The isothermal magnetization curves of x = 0 and doped composites x = 0.04 and x = 0.06 annealed at 600 and 800 °C temperatures.

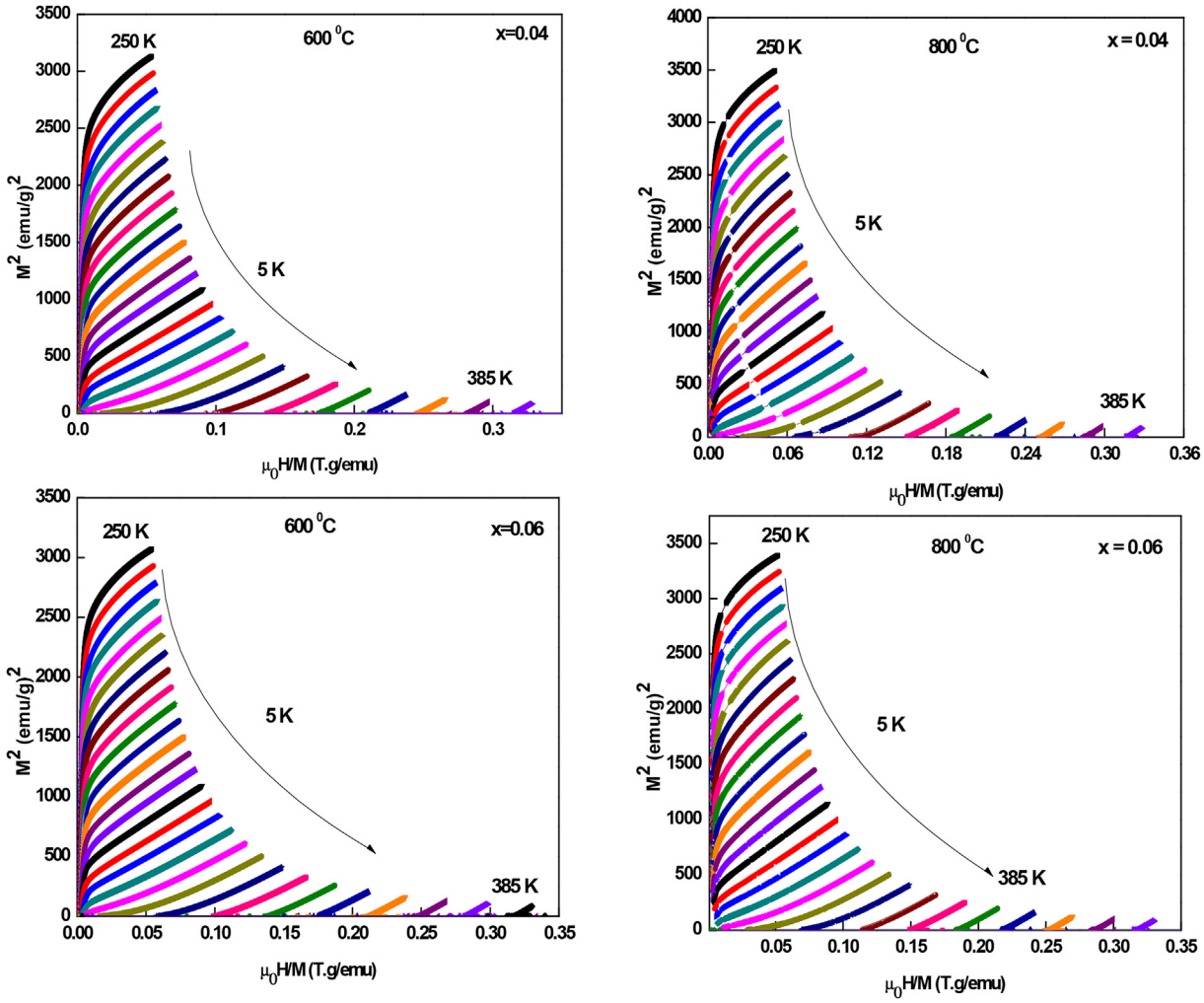

Fig. 5. Arrott plots of LBMO/xTiO$_2$ doped composites x = 0.04 and x = 0.06 composites at 600 and 800 °C annealing temperatures.

isothermal magnetization curves using the approximated Maxwell equation Eq. (1) [18], where, M_{i+1} and M_i are the magnetization values measured at T_{i+1} and T_i temperatures in magnetic field ΔH. In Fig. 6, composites show a broad peak of ΔS around T_c in both annealing temperatures that increases monotonically with the applied magnetic field. In principal, the change in ΔS depends on the change in the intrinsic properties of LBMO, which are kept without any change due to the TiO_2-LBMO interaction lack. This explains the negligible change in the maximum value of ΔS (ΔS_{max}) with annealing temperature for doped composites as shown in Table 3. The effect of annealing temperature appears clearly through the change in the ΔS curves width that can be expressed interms of the full width at half maximum (δT_{FWHM}), where, increasing annealing temperature has been found to increase the δT_{FWHM} of doped composites as seen in Table 2 for 2T applied magnetic field.

$$\Delta S\,(T, \Delta H) = \sum \frac{M_i - M_{i+1}}{T_i - T_{i+1}} \Delta H \tag{1}$$

$$RCP = \Delta S_{Max} \times \delta T_{FWHM} \tag{2}$$

$$\Delta S = a(\mu_0 H)^n \tag{3}$$

Depending on ΔS_{max} and δT_{FWHM}, the magnetocaloric efficiency can be determined through the relative cooling power (RCP) in Eq. (2) [11]. The MCE results show an improvement at the same temperature range with changing annealing temperature, where, the RCP values of doped composites show an enhancement with increasing annealing temperature as seen in Fig. 7a, b. The enhancement in RCP valuesis more likely referring to the enhancement in δT_{FWHM} rather than ΔS_{max} due to the negligible change of ΔS_{max} with changing annealing temperature. This concludes that the change in the magnetocaloric properties of *magnetoresistive/insulator* systems mainly comes from the change in δT_{FWHM} more than ΔS_{max}. From these results, we can draw two important notes, the first one is that TiO_2 addition enhances the MCE properties of LBMO compound at the same temperature range and this has been discussed in details in our previous study [3]. The second note is that annealing process at the higher temperature of 800 °C exhibits interesting results more than 600 °C that may increase the motivation for additional studies at higher temperatures.

As the second order transition has been proved for composites in both annealing temperatures, so, the magnetic field dependence of ΔS should vary according to Eq. (3) [18], where ***a*** is a constant and ***n*** power depends on the magnetic state of the sample. The mean field theory has predicted the 0.67 value for ***n***

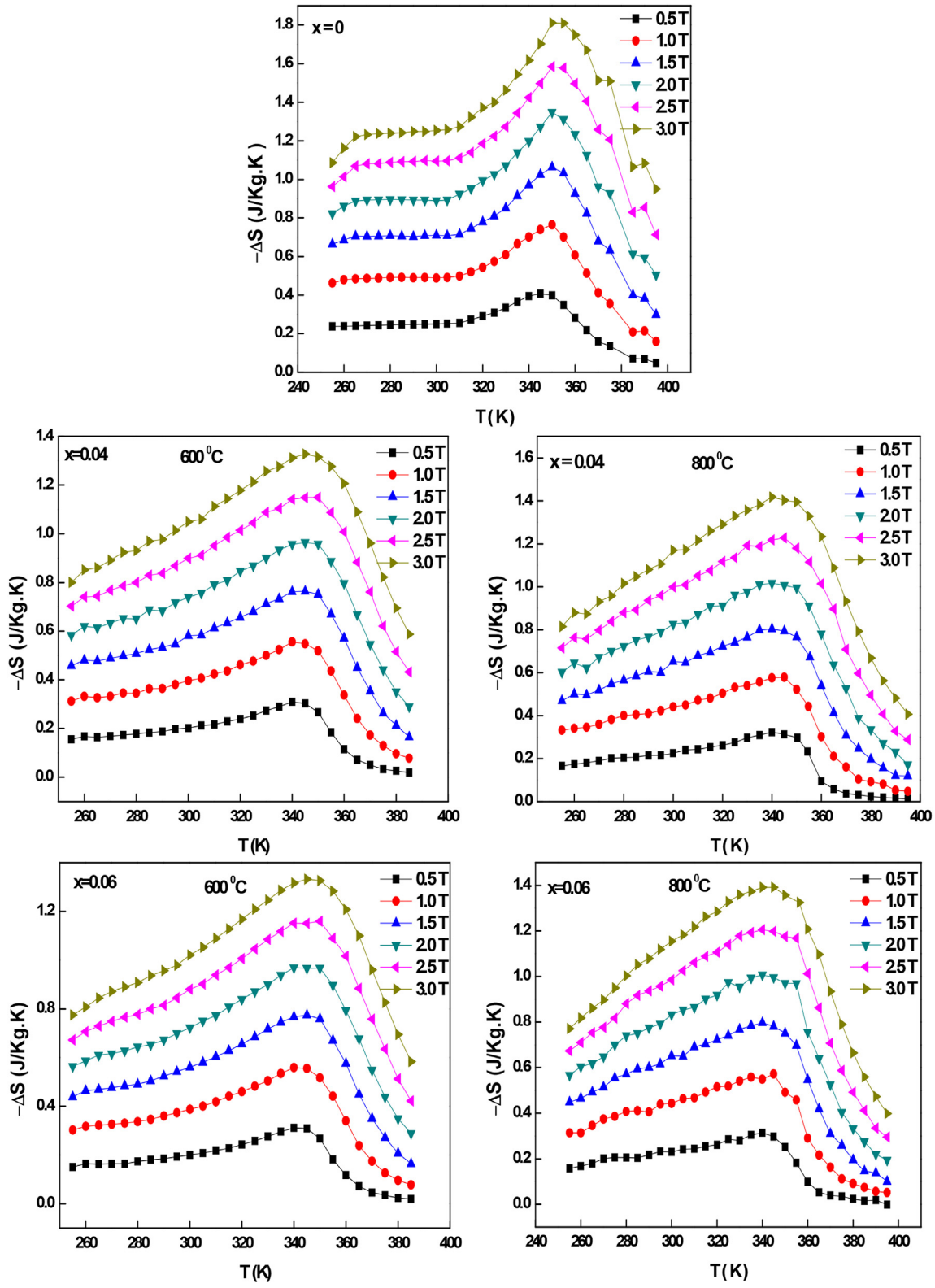

Fig. 6. Thermal variation of magnetic entropy change at different magnetic fields of x = 0 and doped composites of x = 0.04 and x = 0.06 at 600 and 800 °C annealing temperatures.

Table 3
ΔS_{max} (J/kg.K), δT_{FWHM} (K), RCP (J/kg) at 2T and ***n*** exponent of composites annealed at 600 and 800 C.

Composition	Condition	ΔS_{max} (J/kg.K)	δT_{FWHM} (K)	RCP(J/kg)	*n*
X = 0	as-prepared	−1.34	30.15	40.66	0.7
x = 0.04	600 °C	−0.96	53	50	0.95
	800 °C	−1.001	62	62	0.87
x = 0.06	600 °C	−0.966	54	52	1.02
	800 °C	−1.006	66	66	0.87

at T_c [n (T_c)] [19], however, some manganites do not match well with this value [20]. The temperature dependence of ***n*** exponent is displayed in Fig. 7c and d for composites in different annealing temperatures. These figures show the rough decrease of ***n*** value with temperature elevation, passing through a minimum near T_c then increases sharply above T_c. In spite of the close value of ***n***(T_c) in both annealing temperatures to these reported in manganites and rare earth metal materials [21,22], but, there is a notable deviation from the mean field theory value (see Table 3).

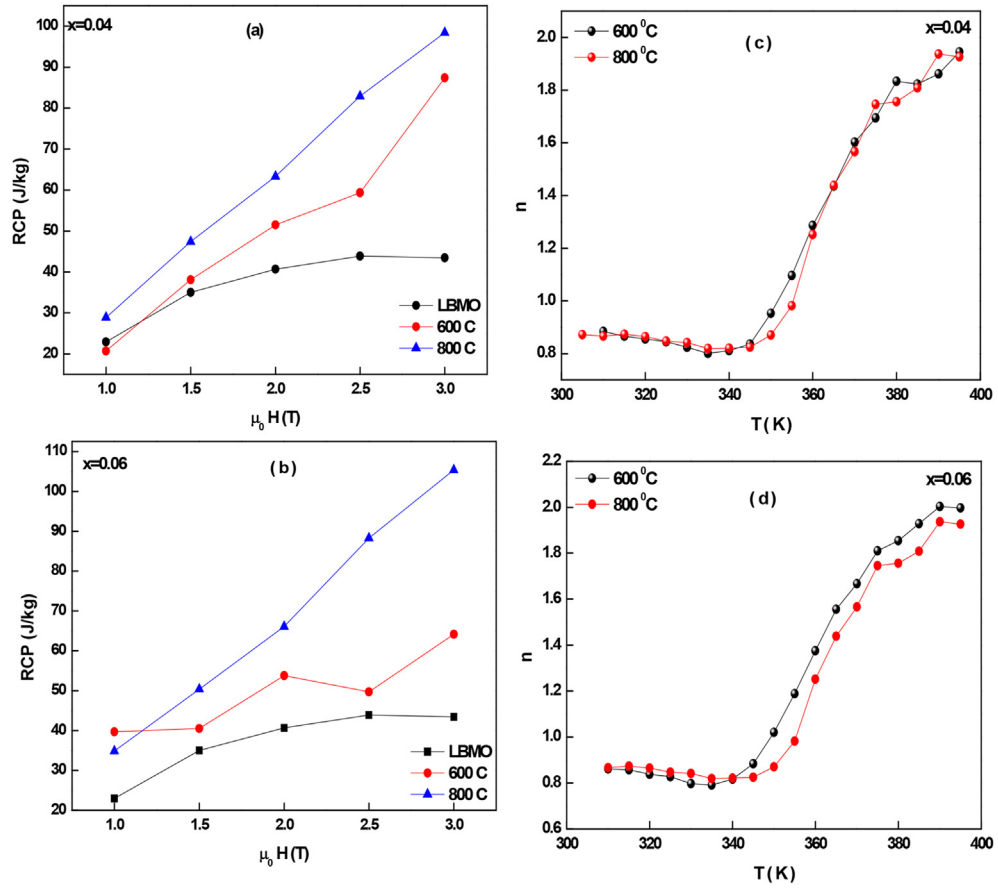

Fig. 7. (a), (b) The variation of RCP with magnetic field and (c), (d) **n** exponent versus temperature for x = 0.04 and x = 0.06 composites annealed at 600 and 800 °C annealing temperatures.

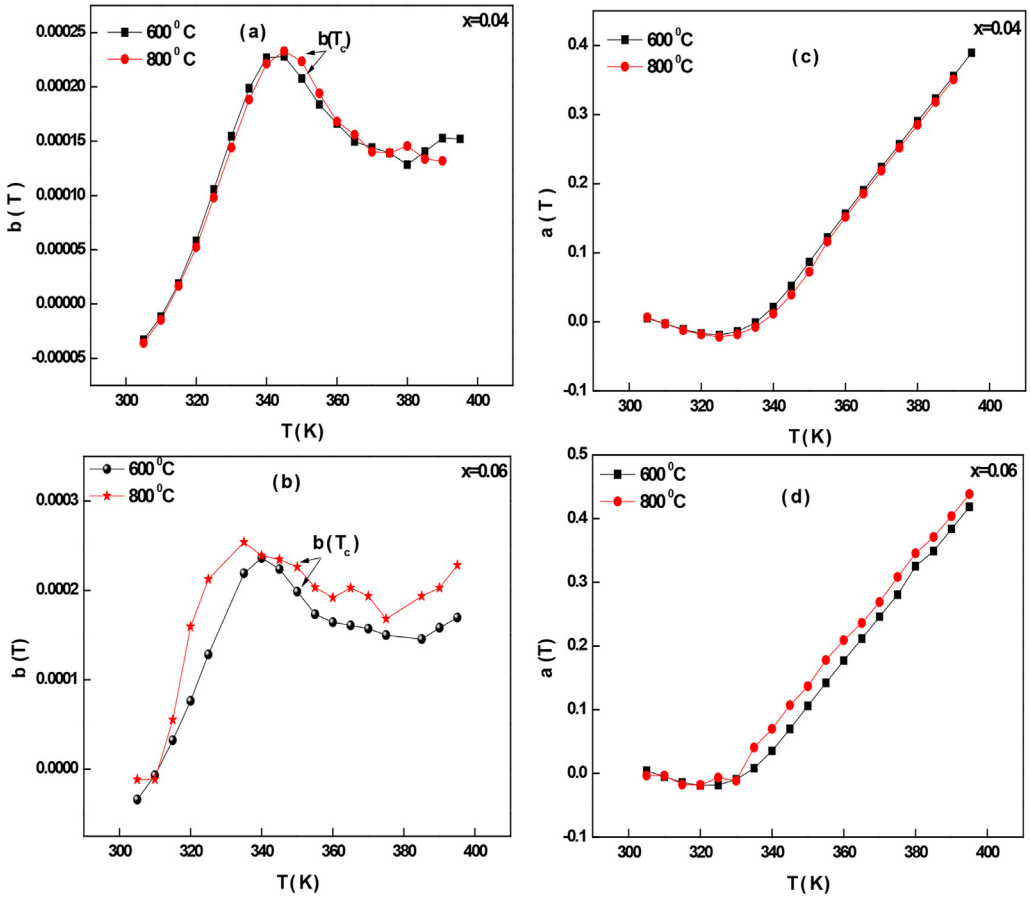

Fig. 8. (a, b) and (c, d) The thermal variation of ***b*** and ***a*** coefficients, respectively, for the x = 0.04 and x = 0.06 composites annealed at 600 and 800 °C.

This difference in value may refer to the local inhomogeneity or the superparamagnetic clusters near T_c [23,24]. Also, it is noteworthy that ***n*** value of doped composites annealed at 800 °C is closer to the mean field theory value than ones annealed at 600 °C, which indicates the enhancement in the local inhomogeneity or in the superparamagnetic clustering at the 800 °C composites.

To identify the participated components in the MCE or its origin, we have modeled the experimental results of MCE with Landau theory [25], which taking into account elastic, magnetoelastic and magnetoelectronic coupling effects. According to this theory, the magnetic energy (**M**) can be involved in Gibb's free energy (**G**) as in Eq. (4), where **a**, **b** and **c** are the temperature dependent Landau thermodynamic coefficients that have been determined at the equilibrium state of Eq. (4) ($\delta G/\delta T = 0$).

$$G(M,T) = G_0 + \frac{a(T)}{2}M^2 + \frac{b(T)}{4}M^4 + \frac{C(T)}{6}M^6 + \ldots\ldots\ldots - \mu_0 H \tag{4}$$

$$-S_M(T,\mu_0 H) = \left(\frac{\delta G}{\delta T}\right)\mu_0 H = \left(\frac{a}{2}\right) + \frac{\delta M^2}{\delta T} + \left(\frac{b}{4}\right)\frac{\delta M^4}{\delta T} + \left(\frac{c}{6}\right)\frac{\delta M^6}{\delta T} \tag{5}$$

In principal, **a** and ***b*** coefficients play important role in ΔS of manganites [20] and can give information about the related magnetic properties. For example, the positive value of ***b*** at T_c, ***b*(T_c)**, indicates the second order transition [25,26] for doped composites in both annealing temperatures as seen in Fig. 8a and b confirming the results obtained from Arrott plots. Also, **a(T)** coefficient in Fig. 8c and d is positive [27] and shows a minimum at T_c around 330 K, which is far from the experimental value.

The calculations of ΔS based on Landau theory are obtained using Eq. (5) that results from Gibb's energy differentiation with respect to temperature. Fig. 9 shows these calculations in comparison with the experimental results of Maxwell equation. The observed difference between them agrees with [28], and indicates

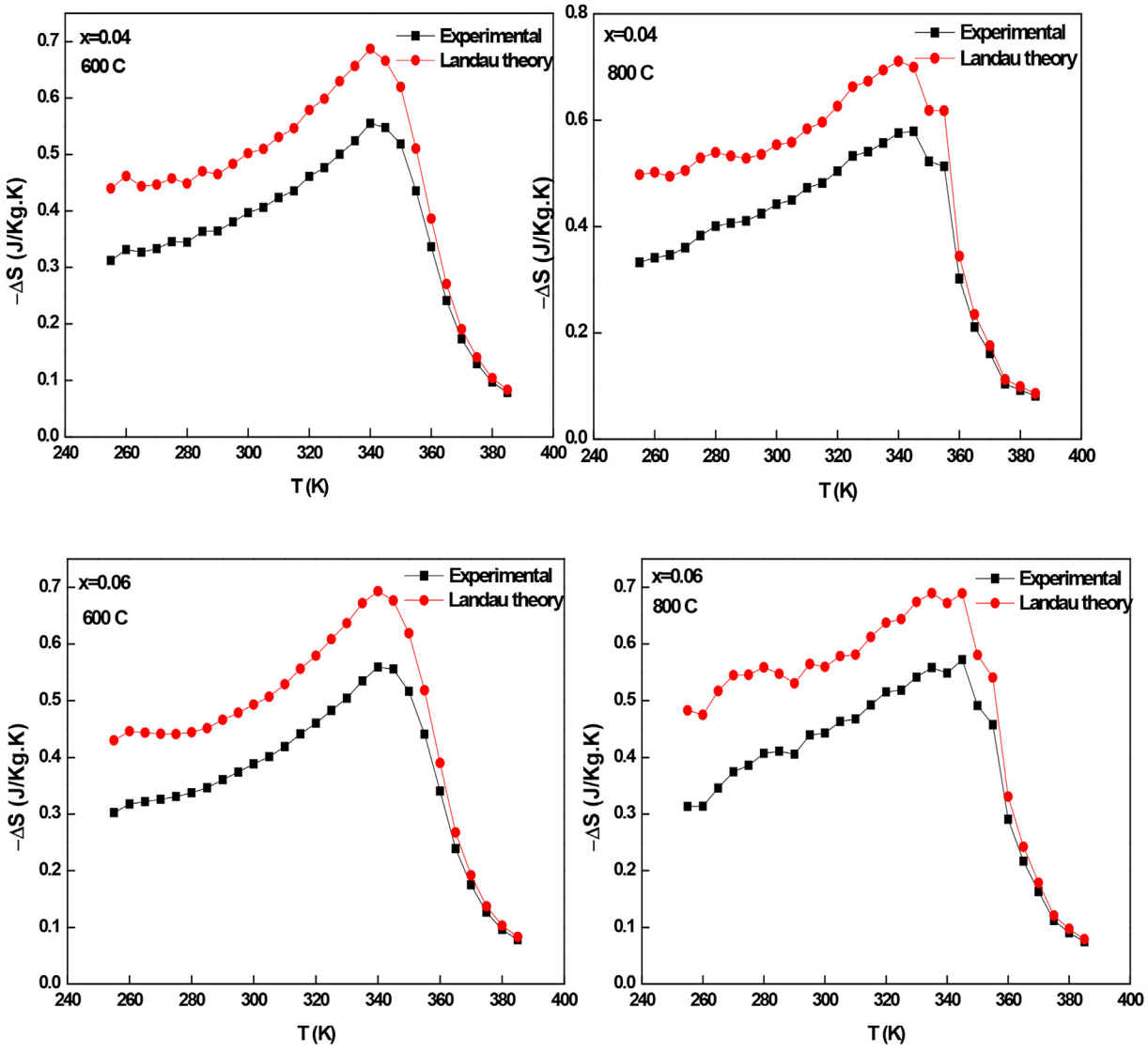

Fig. 9. Experimental and Landau based calculation of ΔSat magnetic field of 1T, for the x = 0.04 and x = 0.06 composites annealed at 600 and 800 °C.

that the magnetocaloric properties arise only due to the magnetic entropy change. This suggests the non contribution of elastic, magnetoelastic and magnetoelectronic coupling, which are involved in Landau theory. And this may be the reason for the different theoretical and experimental T_c values.

4. Conclusions

Structural, magnetic and magnetocaloric properties of $La_{0.7}Ba_{0.3}MnO_3/xTiO_2$ system with x = 0.04 and x = 0.06 composites have been studied as a function of annealing temperature at 600 and 800 °C. The interaction lack between TiO_2 and LBMO preserves the intrinsic properties of LBMO without any change as the R-3c rhombohedral structure and the T_c. TiO_2 distribution in doped composites is affected by annealing temperature, leading to a change in the grain boundaries resistance that affects magnetization pinning. The magnetocaloric properties of doped composites are enhanced at the same temperature range with increasing annealing temperature, where the RCP increases from 50 to 62 J/kg for x = 0.04 composite and from 54 to 66 J/kg for x = 0.06 composite with increasing annealing temperature from 600 to 800 °C. Else, the theoretical calculations of Landau based theory indicate the absence of elastic, magnetoelastic and magnetoelectronic coupling contributions in the magnetocaloric properties.

Acknowledgment

This work was financially supported by the Spanish MINECO Ref. MAT201347231-C2-1-P and MAT2013-48054-C2-2-R, by the Asturias Government Ref. FC-15-GRUPIN14-085 research projects. Authors would like to acknowledge the Egyptian Ministry of Higher Education, technical and human support provided by SGIker Magnetic Measurements Gipuzkoa of UPV/EHU and by University of Oviedo SCT's.

References

[1] A.M. Tishin, Y.I. Spichkin, The Magnetocaloric Effect and its Applications, IOP Publishing Ltd, Bristol, 2003.
[2] A.M. Ahmed, H.F. Mohamed, A.K. Diab, A.A. Mohamed, A.E.A. Mazen, A.M. Mohamed, Indian J. Phys. 89 (2015) 561.
[3] A.A. Mohamed, V. Vega, M. Ipatov, A.M. Ahmed, B. Hernando, J. Alloy Compd. 657 (2016) 495.
[4] H. Hwang, S.W. Cheong, N.P. Ong, B. Batlogg, Phys. Rev. Lett. 77 (1996) 2041.
[5] N.A. Shah, P.S. Solanki, R. Ashish, D.G. Kuberkar, Appl. Nanosci. 5 (2015) 135.
[6] V. Vega, M.A. Cerdeira, V.M. Prida, D. Alberts, N. Bordel, R. Pereiro, F. Mera, S. García, M.H. Vélez, M. Vázquez, J. Non-Cryst. Solids 354 (2008) 5233.
[7] C.V. Vazquez, M.C. Blanco, M.A.L. Quintela, R.D. Sanchez, J. Rivas, S.B. Oseroff, J. Mater. Chem. 8 (1998) 991.
[8] H.J. Kim, S.I. Yoo, J. Alloy. Compd. 521 (2012) 30.
[9] S. Karmakar, S. Taran, B.K. Chaudhuri, H. Sakata, C.P. Sun, C.L. Huang, H.D. Yang, J. Phys. D. Appl. Phys. 38 (2005) 3757.
[10] G. Venkataiah, P.V. Reddy, J. Magn. Magn. Mater 285 (2005) 343.
[11] S. Othmani, M. Bejar, E. Dhahri, E.K. Hlil, J. Alloy. Compd. 475 (2009) 46.
[12] R. Dhahri, F. Halouni, J. Alloy. Compd. 381 (2004) 21.
[13] R.N. Bhowmik, A. Poddar, R. Ranganathan, C. Mazumdar, J. Appl, Phys. 105 (2009) 113909.
[14] R.N. Bhowmik, J. Magn. Magn. Mater 323 (2011) 311.
[15] I.P. Muthuselvam, R.N. Bhowmik, J. Alloy. Compd. 511 (2012) 22.
[16] O.A. Shlyakhtin, K.H. Shin, Y.J. Oh, J. Appl. Phys. 91 (2002) 7403.
[17] S.K. Banerjee, Phys. Lett. 12 (1964) 67.
[18] V.K. Pecharsky Jr., K.A. Gschneidner, J. Appl. Phys. 86 (1999) 565.
[19] H. Oesterreicher, F.T. Parker, J. Appl. Phys. 55 (1984) 4334.
[20] V. Franco, A. Conde, Int. J. Refrig. 33 (2010) 465.
[21] V. Franco, C.F. Conde, A. Conde, L.F. Kiss, Appl. Phys. Lett. 90 (2007) 052509.
[22] V. Franco, J.S. Blazquez, A. Conde, Appl. Phys. Lett. 89 (2006) 222512.
[23] V. Franco, J.S. Blazquez, A. Conde, Appl. Phys. Lett. 100 (2006) 064307.
[24] M. Pekala, J. Appl. Phys. 108 (2010) 113913.
[25] L.D. Landau, E.M. Lifshitz, Statistical Physics, Pergamon, Oxford, 1967.
[26] V.S. Amaral, J.S. Amaral, J. Magn. Magn. Mater 272 (2004) 2104.
[27] J. Inoue, M. Shimizu, J. Phys. Lett. 85 (1982) A90.
[28] A. Mleiki, S. Othmani, W.C. Koubaa, M. Koubaa, A. Cheikhrouhou, E.K. Hlil, J. Alloy Compd. 645 (2015) 559.